Inhibition of migration and invasion of carcinoma cells by urokinase-derived antagonists of αvβ5 integrin activation

ARTICLE *in* INTERNATIONAL JOURNAL OF CANCER · JANUARY 2009

Impact Factor: 5.09 · DOI: 10.1002/ijc.23933 · Source: PubMed

Int. J. Cancer: **124,** 316–325 (2009)

Inhibition of migration and invasion of carcinoma cells by urokinase-derived antagonists of αvβ5 integrin activation

Immacolata Vocca[1], Paola Franco[1], Daniela Alfano[1], Giuseppina Votta[1], Maria Vincenza Carriero[2], Yeriel Estrada[3], Mario Caputi[4], Paolo A. Netti[5], Liliana Ossowski[3] and Maria Patrizia Stoppelli[1]*

[1]*Institute of Genetics and Biophysics "Adriano Buzzati-Traverso", National Research Council, Via Castellino, 111, Naples, Italy*
[2]*Department of Experimental Oncology, National Cancer Institute of Naples, Naples, Italy*
[3]*Department of Materials and Production Engineering, University "Federico II", Naples, and Italian Institute of Technology, Genoa, Italy*
[4]*Department of Medicine, Mount Sinai School of Medicine, New York, NY*
[5]*Department of Medical-Surgical, Cardiological, Respiratory, and Thoracic Sciences, Second University of Naples, Naples, Italy*

We previously showed that, while binding to urokinase receptor (uPAR) through its growth factor domain (GFD, residues 1–49), urokinase (uPA) can engage αvβ5 integrin through an internal domain (CP, residues 132–158). This novel uPA/αvβ5 interaction promotes cytoskeletal rearrangements and directional cell migration (Franco et al., J Cell Sci 2006;119:3424–34). We now show that treatment of cells with phosphomimic uPA (uPA$^{138E/303E}$, serine 138 and 303 substituted with glutamic acid) strongly inhibits matrix-induced cell migration. Unlike uPA, binding of uPA$^{138E/303E}$ to cell surface did not induce F-actin enriched protruding structures and caused a 5-fold reduction in cell translocation speed, as determined by video tracking of living cells. Inhibition of migration was found to be independent of uPAR, since uPA variants lacking the GFD domain, but carrying the relevant Ser to Glu substitutions were as effective inhibitor as uPA$^{138E/303E}$. Through several independent approaches, we established that the phosphomimics specifically bind to αvβ5 integrin through the CP region carrying the S138E mutation. This interaction blocks integrin activation, as determined by a decreased affinity of αvβ5 to vitronectin and a reduced association of the β5 cytoplasmic tail with talin. Finally, stable expression of uPA$^{138E/303E}$ in human squamous carcinoma cells prevented tumor cell invasion *in vivo*. Thus, when expressed in cancer cells, the inhibitory phosphomimic effect was dominant over the effect of endogenously produced uPA. These results shed light on the regulation of cell migration by uPA phosphorylation and provide a realistic opportunity for a novel antiinvasive/metastatic therapeutic intervention.

Key words: uPA phosphorylation; cell migration inhibitor; αvβ5 antagonist; cell cytoskeleton; *in vivo* carcinoma invasion

The ability of tumor cells to cross tissue barriers and invade surrounding tissues is a hallmark of malignant dissemination. Understanding the molecular mechanisms underlying the establishment of the metastatic phenotype is a prerequisite for identifying new pharmacological targets and designing novel therapeutic strategies. In general terms, the metastatic ability of tumor cells is sustained by the local availability of migration-inducing factors and matrix-degrading enzymes, leading to an increased cell migration and tissue invasion. Prominent among the molecular systems involved is the urokinase (uPA)/receptor (uPAR) system, which is overexpressed in many human neoplastic conditions and is linked to an unfavorable clinical outcome.[1] Recent evidence shows that plasma levels of uPA and uPAR are significantly elevated in patients with prostate carcinomas, that they are associated with the development of distant metastases and that they significantly decline after prostate removal.[2] Many antibodies or small inhibitory molecules targeting the uPA/uPAR system are currently under development.[3]

The uPAR consists of 3 cysteine-rich domains (DI, DII, DIII) connected by short linker regions and associated with the membrane through a C-terminal glycosyl-phosphatidyl-inositol anchor. The crystal structure of the uPAR complexed with the uPA amino-terminal fragment (residues 1–135) or with an antagonist peptide shows a deep internal cavity where the ligand inserts, thus leaving the external receptor surface accessible for protein–protein interactions.[4–6]

Increasing evidence shows that uPAR signals through the association with transmembrane receptors like the G-protein-coupled receptor FPR and FPRL1 (formyl peptide receptor 1), the rafts-associated caveolin and EGFR, and integrins such as α5β1, αvβ3, αvβ5, αMβ2 and CD11b/CD18.[7,8] Integrins are a class of adhesion receptors that link the extracellular matrix (ECM) to the cytoskeleton and can either convey ECM signals to cells ("outside-in signaling") and/or sense the status of cytoskeleton and associated proteins ("inside-out signaling"). In mammalian cells, integrins consist of an α and β subunit, and each heterodimer has unique binding specificity and signaling properties.[9]

The ability of uPAR to modify integrin activity as well as integrin-dependent signaling implies that the uPAR is a cis-acting integrin regulator.[10–12] The DI domain of uPAR is required for uPAR/integrin association and signaling.[13,14] At least in 1 case, the uPAR-integrin interaction site has been mapped within the α5 propeller (residues 242–246) of α5β1.[15] Of interest to the current study is uPAR association with αvβ5, which is promoted by uPA or ATF binding to uPAR.[11] Moreover, αvβ5 protein levels are upregulated by uPAR engagement with uPA, suggesting a functional interdependence of these 2 receptors.[16]

The serine protease uPA consists of 2 disulfide-bridge-linked polypeptide chains, an N-terminal A chain (residues 1–158), containing a "growth factor-like" domain (GFD, residues 1–49), a kringle domain (residues 50–131), a "connecting peptide" region (CP, residues 132–158) and a large C-terminal serine protease polypeptide (residues 159–411). The two-chain active enzyme results from a single proteolytic cleavage at Ile^{157}-Lys^{158} of the proenzyme (pro-uPA)-secreted form.[17] Binding to the uPAR occurs through the GFD and is retained by a peptide corresponding to the uPA residues 12–32.[18] Recent findings show that uPA may also bind directly to αvβ5 through a GFD-independent interaction involving the CP region. This association stimulates cell migration and cytoskeletal rearrangements in uPAR-bearing cells.[19–21] The CP region includes Ser^{138}, which is phosphorylated

Additional Supporting Information may be found in the online version of this article.

Abbreviations: Col, collagen; CP, uPA connecting peptide region (residues 132–158); CPp, peptide corresponding to uPA residues 135–158; FN, fibronectin; GFD, uPA growth factor-like domain (residues 1–49); GFDp, peptide corresponding to uPA residues 12-32; LN, laminin; uPA, urokinase; uPAR, urokinase receptor; VN, vitronectin.

Grant sponsor: European Union Framework Programme 6; Grant number: LSHC-CT-2003-503297; Grant sponsor: USPHS Research; Grant number: CA-40578; Grant sponsor: Italian Association for Cancer Research (AIRC); Grant sponsor: Samuel Waxman Cancer Research Foundation.

***Correspondence to:** Institute of Genetics and Biophysics "Adriano Buzzati-Traverso", Via Castellino 111, 80131 Naples, Italy.
Fax: +39-081-6132720 or +39-081-6132706. E-mail: stoppell@igb.cnr.it

Received 7 March 2008; Accepted after revision 6 August 2008
DOI 10.1002/ijc.23933
Published online 9 October 2008 in Wiley InterScience (www.interscience.wiley.com).

in the A431 human carcinoma cell line.[22] This modification neither affects plasminogen activation nor the high affinity binding to the uPAR. However, phosphorylated uPA, as well as a phosphomimic uPA variant (uPA$^{138E/303E}$), lack the ability to stimulate cell migration, paxillin redistribution and p56/59Hck activation,[23,24] but the mechanism underlying the lack of migration-stimulating ability is unknown.

Here, we show that phosphomimic uPA inhibits F-actin enriched cell protrusions, reduces cell migration speed by 5-fold and blocks *in vivo* carcinoma cell invasion. These effects are mediated by specific binding of phosphomimic uPA to the αvβ5 integrin through the CP region, which results in the blockade of integrin activation.

The inhibitory activity of very low concentrations of phosphomimic uPA may suggest new therapeutic antimetastatic strategies and provide a mechanistic model for anticancer drugs targeting integrin receptors.

Material and methods

Reagents

Polyclonal and clone 2 monoclonal anti-uPA antibodies were a gift of P. A. Andreasen, Aarhus, Denmark. β1 integrin polyclonal kit, purified αvβ5 and α1β1 integrin, VNR147 anti-αv, AB1926 anti-β5 and P1F6 anti-αvβ5 monoclonal antibodies were from Chemicon Int. Inc. (Temecula, CA). N-19 goat anti-αv polyclonal antibody was from Santa Cruz (Santa Cruz, CA). Protein G, rhodamine-conjugated phalloidin, FITC-conjugated antibodies, anti-talin clone 8d4, anti α-tubulin monoclonal antibody, collagen (Col), fibronectin (FN) and laminin (LN) were from Sigma (Milan, Italy). Na^{125}I (17.4 mCi/μg), and ^{125}I-UdR (2,200 Ci/mmol) were from Amersham (Piscataway, NJ), and the enhanced chemiluminescence detection system was from Amersham (Milan, Italy). IODO-BEADS were from Pierce (Rockford, IL). COFAL-negative embryonated eggs were obtained from SPAFAS Inc. (North Franklin, CT). All cell culture reagents were purchased from Gibco (Gaithersburg, MD). FuGene6 transfection reagent and Complete™ protease inhibitor cocktail were from Roche diagnostics (Monza, Italy). The pPIC9 vector and Pichia strain GS115 were obtained from Invitrogen Corp. (San Diego, CA). Vitronectin (VN) was from Promega (Madison, WI). Restriction enzymes were from New England Biolabs. Native uPA was from Abbott Laboratories.

The C-terminal histidine-tagged uPA variants shown in Figure 1*a* have been expressed as secreted products in the methylotrophic yeast *P. pastoris* as described.[19]

Plasmids

The αv-pcDNA3 vector was kindly provided by D. Cheresh, UCSD, La Jolla, CA. The pPIC9-His-uPA$^{138E/303E}$ encoding uPA$^{138E/303E}$ was obtained by ligation of a double-strand oligonucleotide (5′-AATTCAGCAATGAACTTCATCAAGTTCCAT and 5′-CGATGGAACTTGATGAAGTTCATTGCTG) to the TaqI-FspI fragment excised from pcDNAneo-His-uPA plasmid and to the NcoI-XbaI fragment from pcDNAneo-His-uPA$^{138E/303E}$.[22] The pPIC9/His-uPA^{138E} was obtained by ligation of the NcoI-AflIII fragment excised from the pPIC9-His-uPA plasmid to the AflIII/NcoI frament excised from pPIC9-His-uPA$^{138E/303E}$ plasmid into the NcoI/NcoI site of the pPIC9 plasmid. To obtain the pPIC9 coding for histidine-tagged ΔGFa$^{138E/303E}$, the region encoding amino acids 66–411 of uPA, included in the 3,099 bp StuI-NcoI fragment and containing the 2 Ser to Glu substitutions was excised from pPIC9-uPA$^{138E/303E}$, ligated into the StuI/NotI sites of pPIC9 multicloning site, together with a double-strand oligonucleotide coding for the first 8 residues of uPA and for amino acids 46–65 (5′GGCCGCGAGCAATGAACTTCATCAAGTTCCAAAGTCA AAAACCTGCTATGAGGGGAATGGTCACTTTTACCGAGGA AAGGCCAGCACTGACAC and 5′CATGGTGTCAGTGCTGGC CTTTCCTCGGTAAAAGTGACCATTCCCCTCATAGCAGGT TTTTGACTTTGGAACTTGATGAAGTTCATTGCTCGC), thus introducing the 9–45 deletion. The uPAR expression vector pcDNA3-uPAR was constructed as described.[19]

Gene silencing

For silencing αv expression, a 25-nucleotide sequence (cctagacgtggacagtcctgccgag) corresponding to nucleotides 985–1010 of αv was introduced into pSUPER vector (pSUPER/αviA). This insert is separated by a 9-nucleotide noncomplementary spacer (tctcttgaa). A control vector (pSUPER/GFPi) was constructed using a 19-nucleotide sequence (gagcgcaccatcttcttca) from the green fluorescent protein (GFP) gene, with no significant homology to any mammalian gene sequence. These sequences were inserted into the pSUPER vector digested with BglII and HindIII.

Peptide synthesis and purification

The peptides employed in this analysis correspond to residues 135–158 of the human uPA sequence (CPp, KKPSSPPEELK FQCGQKTLRPRFK), or to residues 12–32 (GFDp, DCLNGGTA VSNKYFSNIHWCN) and were synthesized as described.[19]

Cell culture and generation of stable transfectants

Human epidermoid carcinoma HEp3 (T-HEp3),[25] tumorigenic and metastatic in the chick embryo and in nude mice,[26,27] was serially transplanted on chorioallantoic membranes (CAMs) and used as a source of tumorigenic cells. T-HEp3, HEK-293 (human embryonic kidney) and the derived stably transfected cell lines were cultured in DMEM with 10% FBS. HEK-293/uPAR-25 and HEK-293/uPAR-12 are described in Ref. 19. All cell lines were grown in the presence of 100 U/ml penicillin and 100 μg/ml streptomycin at 37°C, under 5% CO_2 atmosphere.

To generate stable HEp3 transfectants, a 70% confluent 6-cm dish was incubated with 6 μl of FuGene6 and 1 μg of DNA. For stable HEK-293/αvi transfectants, a semiconfluent 10-cm dish was incubated with 18 μl of FuGene6 and 6 μg of DNA according to the manufacturer's protocol. Cells were then diluted, passaged and selected with the neomycin analogue G418, as described.[22] Secreted uPA from HEp3 clones was quantitated by Western blotting.

Chemotaxis assay

Cells were assayed for directional migration using Boyden chambers, with 8-μm pore size PVPF- filters coated with Col-type IV as described,[19] with minor modifications.

Protein ^{125}I-labeling and radioreceptor binding assay

Two hundred nanograms of ΔGFa$^{138E/303E}$ or VN was labeled with 1 mCi of Na^{125}I using IODO-BEADS in 0.1 M NaP and 0.15 M NaCl pH 7.2 for 10 min at 25°C in a final volume of 100 μl. Specific activity was 20 μCi/μg ΔGFa$^{138E/303E}$, 1 μCi/μg for VN and the ^{125}I-ΔGFa$^{138E/303E}$ preparation retained 70% enzymatic activity. For binding studies, HEK-293 cells (2×10^6/sample) were harvested, acid-treated and incubated with 150,000 cpm of ^{125}I-ligand for 2 hr at 4°C. Under these conditions, cells were exposed to ~0.7 nM of enzymatically active ΔGFa$^{138E/303E}$. For association studies, cells were incubated with ^{125}I-ΔGFa$^{138E/303E}$ for the indicated times. For dissociation studies, cells were preloaded with ^{125}I-ΔGFa$^{138E/303E}$ for 2 hr and incubated in fresh medium for the indicated times. In all cases, acid-extracted specific radioactivity was determined.[28]

Time-lapse video microscopy of single cells

Fifteen thousand HEK-293/uPAR-25 cells were seeded in 35-mm tissue culture plates. After 24 hr, the medium was replaced with serum-free medium containing 1 nM uPA$^{138E/303E}$ or diluents. Dynamics of cell movement was followed by time-lapse cinematography at 37°C and at 5% CO_2, using a specifically designed microscope incubator chamber, placed on an *x, y, z* motorized stage (Prior) of an inverted optical microscope

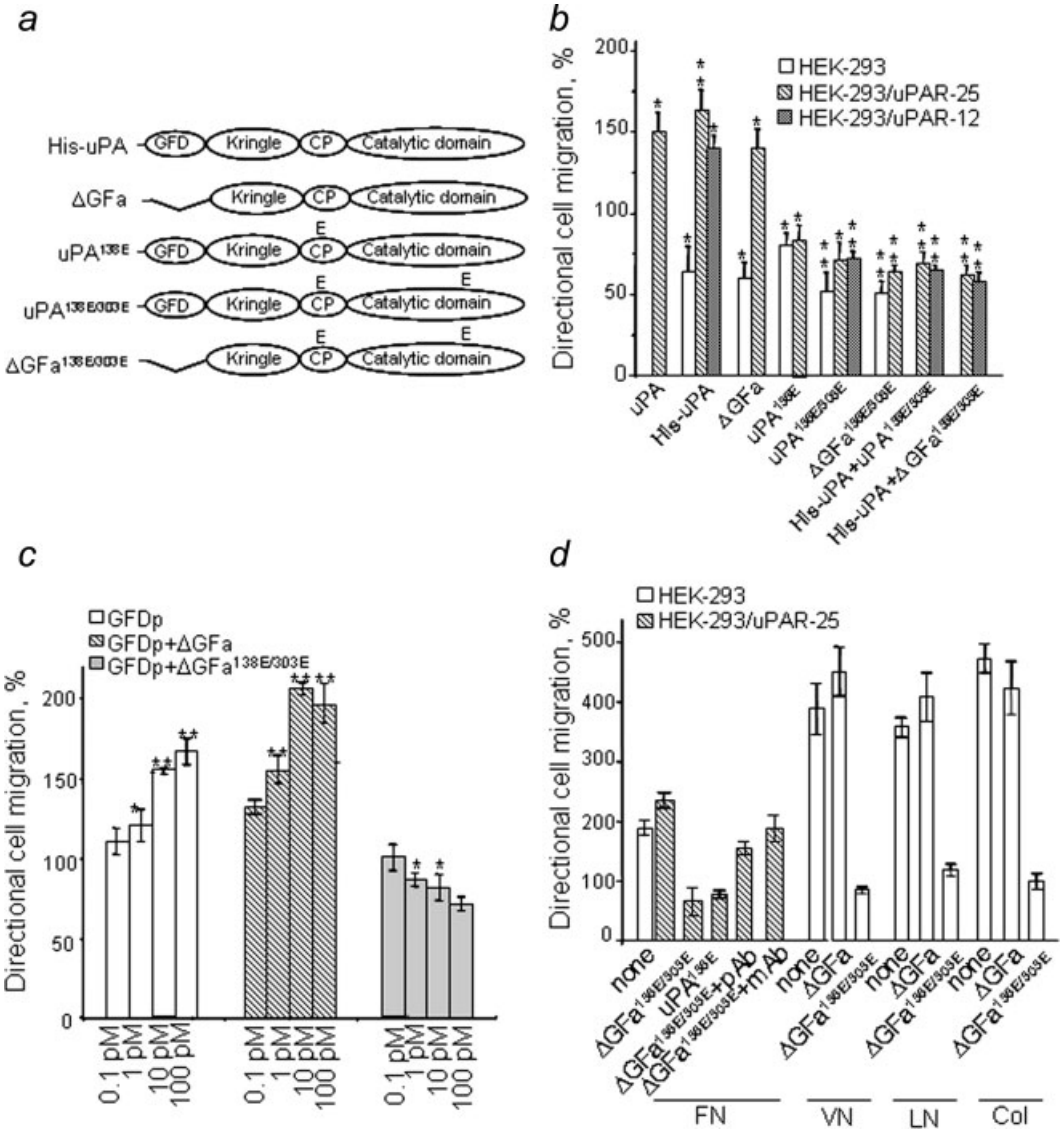

FIGURE 1 – Urokinase receptor-independent inhibition of cell migration by phosphorylated or phosphomimic uPA variants. (*a*) Schematic representation of the human urokinase structure, consisting of a growth factor-like domain (GFD, aminoacids 1–49), a kringle domain (50–131), an interdomain linker region, the connecting peptide (CP, 132–158) and a catalytic domain (159–411). The full-length His-uPA, the mono- (uPA^{138E}) and disubstituted ($uPA^{138E/303E}$) variants, the variants lacking aminoacids 9–45 (ΔGFa and $\Delta GFa^{138E/303E}$) were obtained as C-terminal histidine tagged secreted products in the *P. pastoris* expression system. The His-uPA and the ΔGFa proteins have been described in Ref. 19. (*b*) HEK-293, HEK-293/uPAR-12 and HEK-293/uPAR-25 cells were subjected to a directional migration assay in Boyden chambers using Col-coated filters. 1×10^5 cells/sample were detached by mild trypsinization, incubated in DMEM-10% FBS for 1 hr, acid-treated and allowed to migrate toward 0.1 nM of the indicated uPA variants. When indicated, equimolar concentrations of $uPA^{138E/303E}$ or $\Delta GFa^{138E/303E}$ and His-uPA were employed. Migration in the absence of effectors or random migration was taken as 100%. The results are the average of 3 determinations, with SD indicated by error bars. Statistical analysis was performed with Student's *t*-test. $*p < 0.005$; $**p < 0.0002$. (*c*) HEK-293/uPAR-25 cells were assayed for directional migration toward GFDp or ΔGFa or $\Delta GFa^{138E/303E}$ at the indicated concentrations. In the combinations, a molar ratio of 1:1 was employed. The results are expressed as mean ± SD of 3 independent experiments performed in triplicate. $*p < 0.001$; $**p < 0.00001$. (*d*) HEK-293 and HEK-293/uPAR-25 cells were subjected to a directional migration assay toward 20 μg/ml (FN), 1 μg/ml vitronectin (VN), 5 μg/ml laminin, (LN) or 100 μg/ml collagen (Col). In the combinations, 0.1 nM ΔGFa, $\Delta GFa^{138E/303E}$ or uPA^{138E} were included in the Boyden chamber lower compartment. When indicated, $\Delta GFa^{138E/303E}$ was preincubated with 5 μg/ml of either polyclonal (pAb) or clone 2 monoclonal anti-uPA (mAb) antibodies for 1 hr at 4°C. The results are the average of 3 determinations, with SD indicated by error bars.

(Olympus IX50). Two fields from each dish were selected and scanned sequentially every 6 min for 14 hr at 20× magnification. Images were captured by an Olympus Camera (Coolsnap, Princeton) and analyzed by the Metamorph Imaging software (Metamorph). All the images of a target field were saved in 1 image stack of 180 frames and then analyzed by a cell-tracking routine. Cell migration parameters, *i.e.*, cell speed and persistence length (time span over which the cell moves along a straight line), were evaluated by fitting the (*x, y*) cell coordinates over time to a Lauffenburger-Stokes random walk model using a least-square nonlinear algorithm.[29]

Analysis of cytoskeleton

Cells were harvested by a mild trypsinization, incubated with 10% FBS/DMEM for 1 hr at 37°C, acid-treated and incubated in serum-free medium with the indicated effectors for 1 hr at 23°C. Then cells were then fixed, permeabilized and stained with rhoda-

mine–phalloidin as described.[11] Cells were examined by a Leica microscope (Leica Microsystems, Milan, Italy). At least 3 independent experiments were performed in triplicate, with a minimum of 100 cells observed for each sample.

Invasion of CAM of the chick embryo

Invasion was carried out as described.[30] Briefly, HEp3 human carcinoma cells and the stable transfectants were labeled in culture with 0.2 μCi/ml of ^{125}I-UdR in DME with 5% FBS for 20 hr. The cells were washed extensively, and 300,000 cells in 50 μl PBS were inoculated onto "resealed" CAMs of 10-day-old chick embryos. After 24 hr, noninvading cells were released by trypsinization, and the CAMs were counted in a γ-counter to estimate the number of invading cells. Invasion is expressed as % of cpm found in the CAM before trypsinization and the cpm in the wash (total radioactivity).

β5 integrin/talin coimmunoprecipitation

HEK-293/αv cl.38 cells were seeded onto tissue culture dishes precoated with 5 μg/ml VN or diluents for 1 hr at 37°C. After 18 hr, cells were washed, acid-treated, detached by mild pipetting and incubated with or without 0.1 nM $\Delta GFa^{138E/303E}$ for 1 hr at 37°C. After incubation, cells were lysed in lysis buffer (140 mM NaCl, 50 mM Tris-HCl, pH 7.5, 0.1% SDS, 1% Triton X-100, 1 mM Na_2VO_4 and protease inhibitor mixture). Lysates (200 μg/sample) were precleared with 10 μl Protein G-Sepharose for 1 hr at 4°C, immunoprecipitated with anti-β5 AB1926 antibody, incubated with 15 μl of Protein G-Sepharose and resolved onto a 7.5% SDS-PAGE followed by a Western blotting with clone 8d4 anti-talin monoclonal antibody.

Statistics

The results were analyzed using the Student's *t*-test. A value of $p < 0.05$ was considered to be significant. Data are presented as the mean ± SD, and the number of experiments performed is indicated in the figure legends.

Results

Previous work from this laboratory has shown that phosphorylation of uPA on $Ser^{138/303}$, or substitution of the phosphorylatable serines with glutamic acid residues, abolishes uPA migration-inducing ability.[22]

uPAR-independent inhibition of cell migration by disubstituted uPA

In an effort to characterize the mechanism underlying the inhibitory effect of $uPA^{138E/303E}$ and to determine whether its direct interaction with uPAR is involved in the inhibition, several uPA variants carrying different deletions and/or glutamic acid-substitutions were obtained as histidine-tagged proteins (Fig. 1*a*) and compared to a histidine-tagged wild-type uPA (His-uPA). All products retained enzymatic activity and, with the exception of the ΔGFa and $\Delta GFa^{138E/303E}$ variants, all retained the ability to interact with uPAR (not shown). In this series of experiments, HEK-293 cells transfected with uPAR and stably expressing ~3,000 uPAR/cells (HEK-293/uPAR-12), or ~350,000 uPAR/cells (HEK-293/uPAR-25), were used to test the effect of $uPA^{138E/303E}$ on migration; the parental HEK-293 cells, with undetectable uPAR expression served as controls. As shown in Figure 1*b*, full-length uPA (native and His-tagged) as well as ΔGFa elicited migratory response, only in cells expressing uPAR. There was only a small difference in cell response to His-uPA between clone 12 (low uPAR) and clone 25 (high uPAR). In parental HEK-293 cells, His-uPA caused a slight inhibition of migration, the mechanisms of which we did not explore further. In contrast, when uPA with S138E, or S138E/S303E substitutions, or uPA lacking the uPAR-binding domain but similarly substituted ($\Delta GFa^{138E/303E}$) were used, no migratory responses were elicited in the uPAR-expressing HEK-293 cells. Moreover, both uPA and ΔGFa with the serine substitutions blocked His-uPA induced migration.

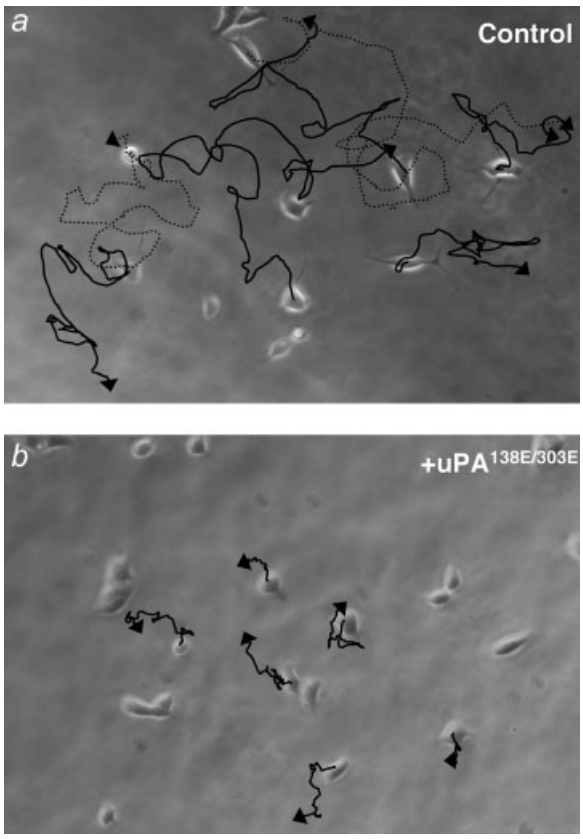

Figure 2 – Video tracking of living cell migration in the presence of the inhibitory $uPA^{138E/303E}$. Cell tracking analysis of the steady-state HEK-293/uPAR-25 cell population in the absence (*a*) or in the presence (*b*) of 1 nM $uPA^{138E/303E}$. Cells were recorded for 14 hr every 6 min while kept at 37°C, under a 5% CO_2 atmosphere. Ten cells/field were followed in a total of 4 fields/sample. Images were analyzed as described in Material and Methods.

Migration-stimulating ability of the intact uPA and the inhibitory ability of the $\Delta GFa^{138E/303E}$ variant suggest that the negative regulatory effect is likely the result of uPA phosphorylation. To investigate this aspect further, the effect of either ΔGFa or $\Delta GFa^{138E/303E}$ on migration elicited by a peptide corresponding to the uPAR binding domain of uPA (GFDp, residues 12–32) was tested. While an equimolar mixture of ΔGFa with GFDp increased migration over that of GFDp alone (Fig. 1*c* and Ref. 19), the substituted $\Delta GFa^{138E/303E}$ completely neutralized GFDp-induced migration, and even inhibited it below the control level. This effect was noticed at concentration as low as 0.1 pM and extended to 10 and 100 pM (Fig. 1*c*). These data show that GFDp-stimulated migration can be inhibited by $\Delta GFa^{138E/303E}$ and that the inhibition is dependent on the 2 Ser to Glu substitutions.

To further characterize the inhibitory activity, the effect of phosphomimic molecules on directional migration of HEK-293 cells toward FN, VN, LN and Col was examined. The unsubstituted molecules had only a minimal, mostly stimulatory, effect on already potent induction of migration by the matrix proteins (Fig. 1*d*). In contrast, both $uPA^{138E/303E}$ and $\Delta GFa^{138E/303E}$ prevented migration toward all effectors, regardless of uPAR expression. Inclusion of monoclonal or polyclonal anti-uPA antibodies relieved the inhibitory effect by ~60%. These results indicate that unique interactions of the phosphomimic uPA molecules exert an inhibitory effect on multiple migration inducers and that this effect is GFD- and uPAR-independent (Fig. 1*d*).

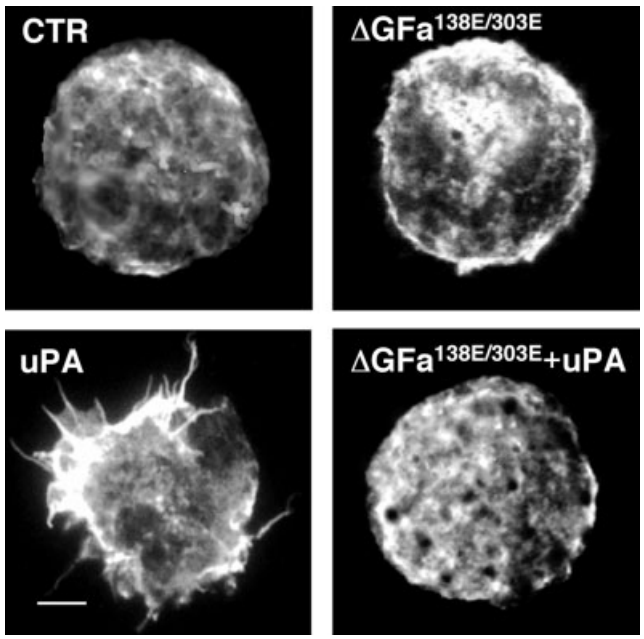

FIGURE 3 – Cytoskeletal rearrangements in HEK-293/uPAR-25 cells exposed to the inhibitory uPA variants. Subconfluent cells were collected by a mild trypsinization, incubated in suspension with 100 pM uPA, 100 pM $\Delta GFa^{138E/303E}$ or equimolar concentrations of uPA and $\Delta GFa^{138E/303E}$ or diluents (CTR) at 0.1 nM for 1 hr at 23°C. F-actin was detected by staining with rhodamine–phalloidin, as specified in the Material and Methods section. In the figure, representative images of HEK-293/uPAR-25 subjected to the indicated pretreatments are shown. Original magnification: ×630. Bar, 5 μm.

Reduction of cell motion speed in the presence of $uPA^{138E/303E}$

To further characterize the inhibitory effect of $uPA^{138E/303E}$, we tested whether the reduced number of motile cells observed in directional migration assay was due to a reduced rate of migration speed. To directly measure distance traveled per time unit, HEK-293/uPAR-25 cells were analyzed in a cell-tracking video-recorded microscopy experiment, in which consecutive frames were taken every 6 min for 14 hr. As shown in Figure 2, the recorded paths of HEK-293/uPAR-25 cells exposed to $uPA^{138E/303E}$ (panel *b*) are appreciably shorter than those of controls (panel *a*). Computational analysis revealed that, compared with control, the presence of $uPA^{138E/303E}$ caused a 5-fold reduction of the average cell speed (2.55 μ/min *versus* 0.55 μ/min, respectively). A slight increase in the persistence length of the cells exposed to $uPA^{138E/303E}$ was also observed (14.3 min *versus* 8.52 min, respectively). Remarkably, the video recordings revealed that $uPA^{138E/303E}$ dramatically impaired the generation and the extension of the multiple outward ruffling filopodia. Representative movies are provided as supplemental material (Movies 1 and 2). Overall, these data show conclusively that phosphomimic uPA inhibits the speed of cell migration.

F-actin redistribution in response to the inhibitory uPA variants

We reasoned that actin reorganization, a crucial prerequisite for lamellipodia and filopodia extension, might be affected by the inhibitory variants. We and others have described the ability of uPA to induce the formation of lamellipodia-type protruding structures.[19–21] Here, HEK-293/uPAR-25 cells were treated for 1 hr with uPA-related proteins, and the cellular distribution of F-actin was analyzed by rhodamine–phalloidin staining (Fig. 3). Following cell exposure to uPA, the mostly cortically distributed F-actin in untreated cells was redistributed, in most cells, into prominent cytoplasmic clusters and protruding structures (Fig. 3). In contrast, in cells exposed to the $\Delta GFa^{138E/303E}$ variant, or to an equimolar combination of uPA and $\Delta GFa^{138E/303E}$, there were no protrusions or F-actin-containing protrusions. Instead, F-actin was punctuate and dispersed within the cell body. These data indicate that the inhibitory $\Delta GFa^{138E/303E}$ lost the ability to reorganize actin into F-actin-enriched protrusions.

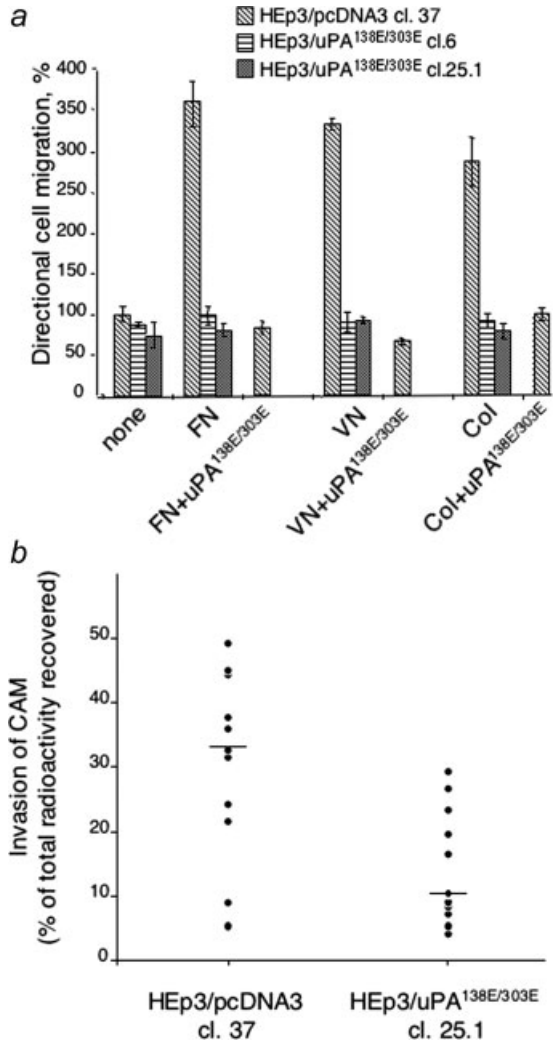

FIGURE 4 – Effect of endogenous $uPA^{138E/303E}$ on HEp3 carcinoma cell migration and CAM invasion. (*a*) Human carcinoma HEp3 cells stably expressing $uPA^{138E/303E}$ (HEp3/$uPA^{138E/303E}$ cl.6, and HEp3/$uPA^{138E/303E}$ cl.25.1) or HEp3 cells bearing pcDNA3 vector (HEp3/pcDNA3 cl.37) were subjected to a directional migration assay in Boyden chambers under serum-free conditions. 10^5 cells/sample were allowed to migrate for 3 hr at 37°C toward 0.1 nM uPA or $uPA^{138E/303E}$ or diluents in combination with FN, VN or Col. Then, cells on the lower side of the filters were counted using an inverted microscope at 10× magnification. Migration of control cells in the absence of effectors or random migration was taken as 100%. Data are presented as the mean ± SD of 3 separate experiments performed in duplicate. (*b*) HEp3/pcDNA3 cl.37 and HEp3/$uPA^{138E/303E}$ cl.25.1 were compared for their ability to invade CAM as described in Material and Methods. Each symbol represents a single CAM. Medians are shown by horizontal bars (32.6 and 10.3, respectively). Statistical analysis was carried out with Student's *t*-test ($p < 0.0002$).

In vivo *inhibition of human carcinoma cell invasion by phosphomimic urokinase ($uPA^{138E/303E}$)*

To test the effect of endogenously produced $uPA^{138E/303E}$ on the behavior of malignant cells in culture and *in vivo*, a highly

malignant HEp3 cell line[25] was transfected either with pcDNA3 vector or with pcDNA3-uPA$^{138E/303E}$ encoding the uPA$^{138E/303E}$ protein.

Several clones (HEp3/uPA$^{138E/303E}$) were selected in which the transgenic, inhibitory uPA was at least equal to, or greater than the endogenous, unsubstituted uPA (not shown). First, in a directional migration assay in Boyden chambers, 100 pM of exogenous uPA$^{138E/303E}$ was added to vector control HEp3 cells (HEp3/pcDNA3 cl.37), which produce ~60 pM uPA during the 3 hr migration assay. This treatment very strongly inhibited HEp3 migration toward FN, VN or Col (Fig. 4*a*) suggesting that even at a lower than equimolar ratio, the substituted uPA has a dominant inhibitory effect. Subsequently, cell migration toward FN, VN or Col was tested in 2 clones producing substituted uPA (HEp3/uPA$^{138E/303E}$ cl.6 and HEp3/uPA$^{138E/303E}$ cl.25.1). As shown in Figure 4*a*, while the vector control clone responded to stimulation by all 3 matrix-proteins with increased migration, no migration was induced by these proteins in either 1 of the 2 uPA$^{138E/303E}$-expressing clones.

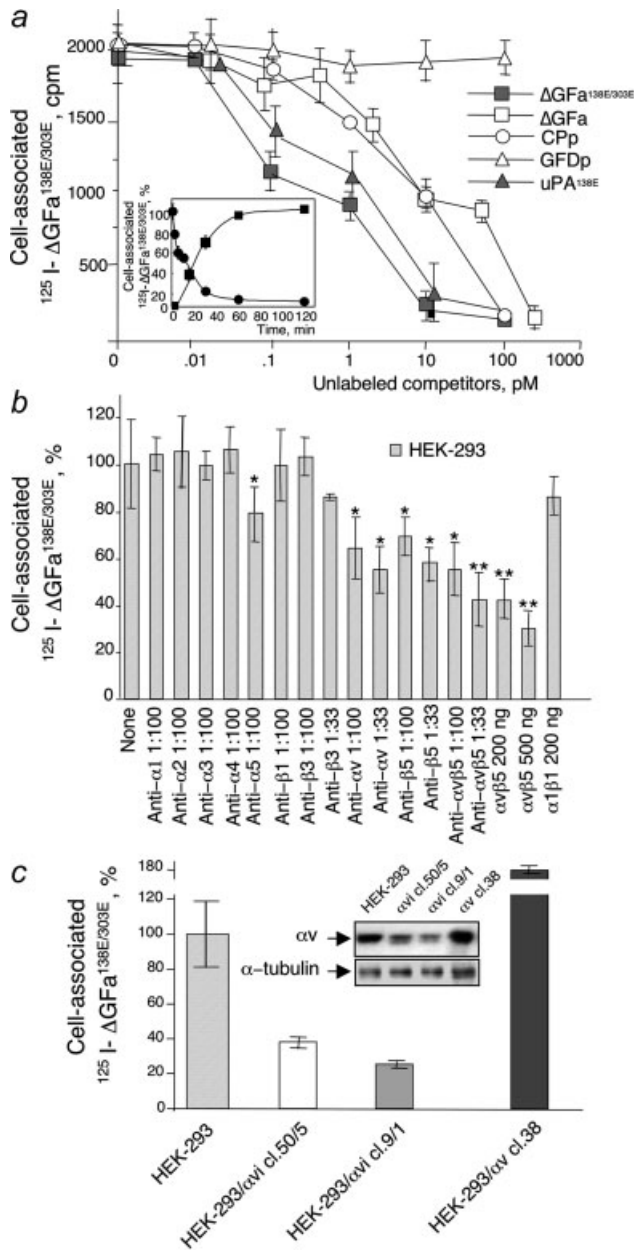

The inhibitory effect of the endogenously produced, substituted uPA, on invasive ability was tested by using HEp3/uPA$^{138E/303E}$ cl.25.1 in an *in vivo* model consisting of a modified chick embryo CAM. In this model, the CAM is wounded and allowed to reseal *in vivo*, a process that recruits to the wounded surface a layer of fibroblasts rich in FN and Col that poses a barrier to invasion. HEp3/uPA$^{138E/303E}$ cl.25.1 or vector-transfected control cells (HEp3/pcDNA3 cl.37), prelabeled with ^{125}I-UdR, were inoculated on CAMs, and their ability to invade was quantified as previously described.[30] The results indicate that expression of the disubstituted, inhibitory uPA, even in the presence of highly expressed native uPA, significantly impairs the ability of malignant cells to spread *in vivo* (Fig. 4*b*).

uPAR-independent specific binding of disubstituted uPA to αvβ5 integrin

We have shown that uPA can engage cell surface through a novel interaction between the CP region (residues 132–158) and αvβ5 integrin.[19] Here, we examine whether ΔGFa$^{138E/303E}$ can also specifically associate with cell surface through the CP region. To test this, ^{125}I-ΔGFa$^{138E/303E}$ was incubated with HEK-293 cells, in the presence or in the absence of indicated, unlabeled competitors for 2 hr at 4°C and the surface-associated radioactivity was measured. Competition binding assays revealed that ΔGFa$^{138E/303E}$ bound with a 10-fold higher affinity than ΔGFa, a property that was shared, to a large degree, by the monosubstituted uPA^{138E} variant. This suggests an important functional role of the region surrounding this phosphorylation site (Fig. 5*a* and Ref. 19). Approximately 10 pM peptide corresponding to residues 135–158 of human uPA (CPp) was sufficient to compete off 50% of the ^{125}I-ΔGFa$^{138E/303E}$ from the cell surface, whereas GFDp was ineffective, suggesting that the disubstituted protein binds to the cell surface through the CP region. To further characterize the binding properties of ^{125}I-ΔGFa$^{138E/303E}$, cells were incubated with ^{125}I-ΔGFa$^{138E/303E}$ for different times. At each time-point, radioactivity specifically associated with the cell surface was determined (inset to Fig. 5*a*). For dissociation studies, cells were first pre-

FIGURE 5 – Specific binding of ^{125}I-ΔGFa$^{138E/303E}$ to αvβ5 integrin on HEK-293 cell surface. In all competition binding assays, ^{125}I-ΔGFa$^{138E/303E}$ (150,000 cpm) was incubated with HEK-293 cells (2×10^6 cells/sample) for 2 hr at 4°C, in the presence of the indicated effectors. After washing, cell-associated radioactivity was eluted and determined by a γ-counter. (*a*) Cells were incubated with ^{125}I-ΔGFa$^{138E/303E}$ in the presence of increasing concentrations of unlabeled ΔGFa$^{138E/303E}$, ΔGFa, uPA^{138E}, CPp or GFDp. Results are presented as the mean of specific binding ± SD, and data are representative of 3 independent experiments performed in duplicate. *Inset*: time-dependent association and dissociation rates of ^{125}I-ΔGFa$^{138E/303E}$ to HEK-293 cell surface at 4°C. (*b*) Cells were pre-incubated with the indicated, antibody dilution for 1 hr at 4°C. When indicated, ^{125}I-ΔGFa$^{138E/303E}$ was pre-incubated either with purified αvβ5 protein (200 or 500 ng) or α1β1(200 ng) for 1 hr before the assay. Nonspecific binding was assessed by including additional duplicate samples containing unlabeled 10 nM ΔGFa$^{138E/303E}$. Specific binding to untreated cells was taken as 100%, and the extent of inhibition by anti-integrin antibodies or by αvβ5 or α1β1 proteins was calculated relative to this value. Results are presented as the mean of specific binding ± SD in percent and are representative of 3 independent experiments performed in duplicate. *$p < 0.05$; *$p < 0.006$. (*c*) In this assay, HEK-293 cells or HEK-293 cells silenced for αv expression (HEK-293/αvi cl. 50/5 and 9/1) or HEK-293 cells overexpressing αv (HEK-293/αv cl. 38) were incubated with ^{125}I-ΔGFa$^{138E/303E}$ in the presence or in the absence of excess unlabeled ΔGFa$^{138E/303E}$ ad described in panel B. *Inset:* One hundred micrograms of total cell lysates from parental HEK-293, HEK-293/αvi cl. 50/5, HEK-293/αvi 9/1 and HEK-293/αv cl.38 were resolved on a 7.5% SDS-PAGE followed by Western blotting with anti-αvβ5 polyclonal (upper panel) and anti-α-tubulin antibodies (lower panel).

loaded with ^{125}I-ΔGFa$^{138E/303E}$, then transferred to unlabeled medium and the extent of acid-extractable radioactivity was assessed at the indicated times. As shown in the inset to Figure 5*a*, 50% association was achieved in ~20 min and cells released 50% of bound material in 15–20 min at 4°C. Overall, these data indicate the occurrence of a high affinity interaction between ^{125}I-ΔGFa$^{138E/303E}$ and HEK-293 cell surface.

To test whether αvβ5 integrin is directly involved in this binding, HEK-293 cells were incubated with ^{125}I-ΔGFa$^{138E/303E}$ after they have been preexposed to a panel of anti-integrin blocking antibodies. The ability of these antibodies to block integrin adhesion to their respective matrix molecules has been tested previously.[19] Only anti-αv, anti-β5 and anti-αvβ5 antibodies caused a 50–60% reduction in the radioactivity specifically associated with the cell surface; antibodies to other integrins had little or no effect (Fig. 5*b*). Moreover, pre-incubation of purified αvβ5 integrin with ^{125}I−ΔGFa$^{138E/303E}$ prior to its addition to HEK-293 cells resulted in a dose-dependent reduction in cell-surface radioactivity. Incubation of ^{125}I−ΔGFa$^{138E/303E}$ with α1β1 integrin, which according to the antibody-blocking experiment was not involved in binding, did not change cell-associated radioactivity (Fig. 5*b*). To demonstrate the involvement of αv integrin more directly, several clones of HEK-293 cells in which αv expression was silenced by transfection of the pSUPER vector engineered to express short hairpin RNAs, were analyzed. HEK-293 cells that harbored the pSUPER vector containing RNAi specific sequences for silencing GFP were selected as a pool and served as control. Of 10 clones analyzed by Western blotting and quantitative densitometry, clone HEK-293/αvi cl.9/1 exhibited a 70% decrease in αv expression and clone HEK-293/αvi cl.50/5 exhibited 30% reduction (Fig. 5*c*, inset). A clone transfected to overexpress αv (HEK-293/αv cl.38,[19]) was used as positive control. As shown in Figure 5*c*, the extent of specific binding of ^{125}I-ΔGFa$^{138E/303E}$ was directly related to the expression level of αv. Taken together, these data indicate that the inhibitory uPA variants (ΔGFa$^{138E/303E}$, uPA$^{138E/303E}$, uPA^{138E}) bind to αvβ5 integrin in an uPAR-independent manner through the CP region.

Activation of αvβ5 integrin is blocked by ΔGFa$^{138E/303E}$

Using a chemotaxis assay, we examined the rate of migration of HEK-293/uPAR-25 cells in response to increasing concentrations of VN. Cell response to VN was dose-dependent and was observed at as little as 1 nM VN. However, while chemotactic response in cells preincubated with ΔGFa for 1hr at 23°C required only 1/10 concentration of VN (0.1 nM) of control cells, to evoke chemotactic response than control cells, cells preloaded with ΔGFa$^{138E/303E}$ required 20- to 50-fold more VN for inducing a similar migration (Fig. 6*a*). We reasoned that ΔGFa$^{138E/303E}$ may directly compete with VN for binding to integrin. To assess that, a binding assay with ^{125}I-VN in the presence of excess unlabeled ΔGFa$^{138E/303E}$ or ΔGFa was set up under the conditions described in Methods. The results showed no reduction of cell-associated ^{125}I-VN in the presence of ΔGFa or ΔGFa$^{138E/303E}$, suggesting that uPA variants and VN do not share the same binding site on integrin (not shown). An alternative explanation of results described in Figure 6*a*, is that preexposure of cells to ΔGFa$^{138E/303E}$ might change the activation state of the VN-binding integrin.

Most integrins become activated following binding to their respective ligands. Rapid changes in affinity as well as cooperative interactions promoted by changes in integrin clustering have been widely documented.[31] We hypothesized that the need for greater VN concentration in the chemotaxis assay is the result of ΔGFa$^{138E/303E}$ blocking αvβ5 in a resting conformation and thus preventing ligand-dependent increase in binding affinity. To test this hypothesis, HEK-293 cells were pretreated with ΔGFa or ΔGFa$^{138E/303E}$ or diluents for 40 min at 25°C and then incubated with ^{125}I-VN at 4°C, in the presence of increasing concentrations of unlabeled VN. As shown in Figure 6*b*, preexposure of HEK-293 cells to ΔGFa$^{138E/303E}$ reduced integrin affinity for ^{125}I-VN by ~10-fold, while pretreatment with ΔGFa resulted in increased affinity. Therefore, the affinity of ^{125}I-VN/integrin interaction may be modulated by the phosphorylation status of the uPA CP region.

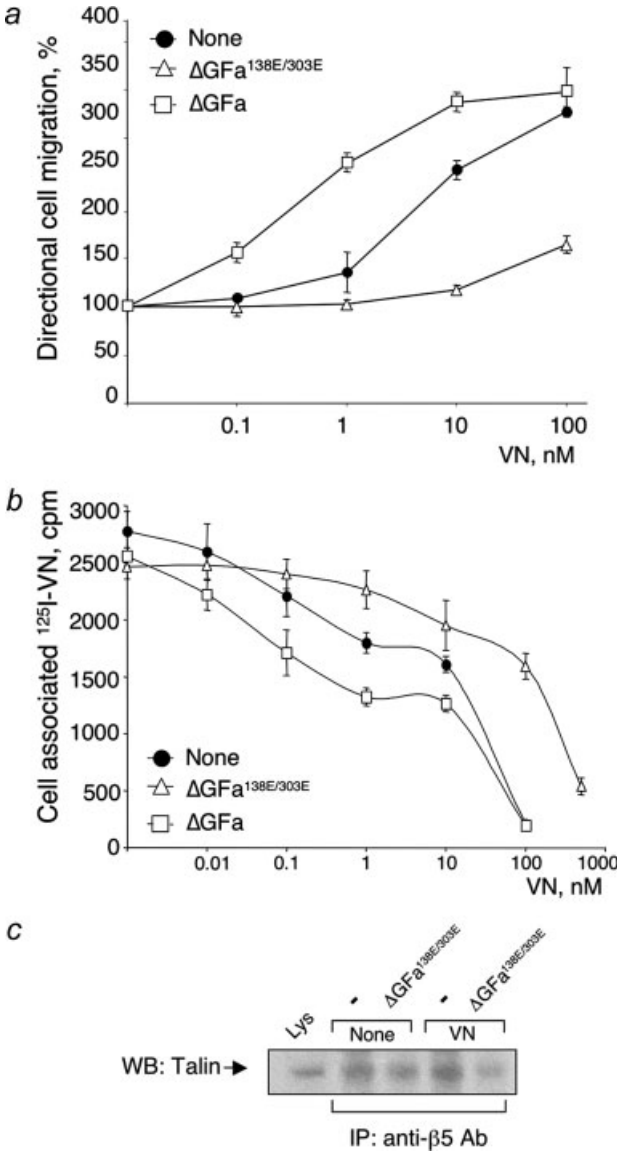

FIGURE 6 – Effect of ΔGFa$^{138E/303E}$ on αvβ5 signaling activity. (*a*) Migration of HEK-293/uPAR-25 cells toward increasing concentrations of VN after 1-hr pretreatment with 0.1 nM ΔGFa$^{138E/303E}$ or ΔGFa or diluents (none). The migration assay was performed as specified in the legend to Figure 1*a*. (*b*) HEK-293 cells (2×10^6) were exposed to 0.1 nM ΔGFa$^{138E/303E}$ or ΔGFa or diluents for 1 hr at 25°C and then incubated for 3 hr at 4°C with ^{125}I-VN (150,000 cpm) in the presence of increasing concentrations of unlabeled VN. Specific cell-associated radioactivity was determined by γ-counting. Results are presented as the mean of specific binding ± SD and are representative of 3 independent experiments performed in duplicate. (*c*) HEK-293/αv cl.38 cells were incubated for 18 hr in tissue culture dishes precoated with VN or with diluents (None) and then incubated with 0.1 nM ΔGFa$^{138E/303E}$ or diluents (−) for 1 hr at 37°C. Cell lysates (200 μg/sample) were immunoprecipitated with anti-β5 polyclonal antibody, and integrin-associated talin was revealed by Western blotting using an anti-talin antibody. Hundred micrograms of total lysate (Lys) from HEK-293/αv cl.38 cells was loaded as a control.

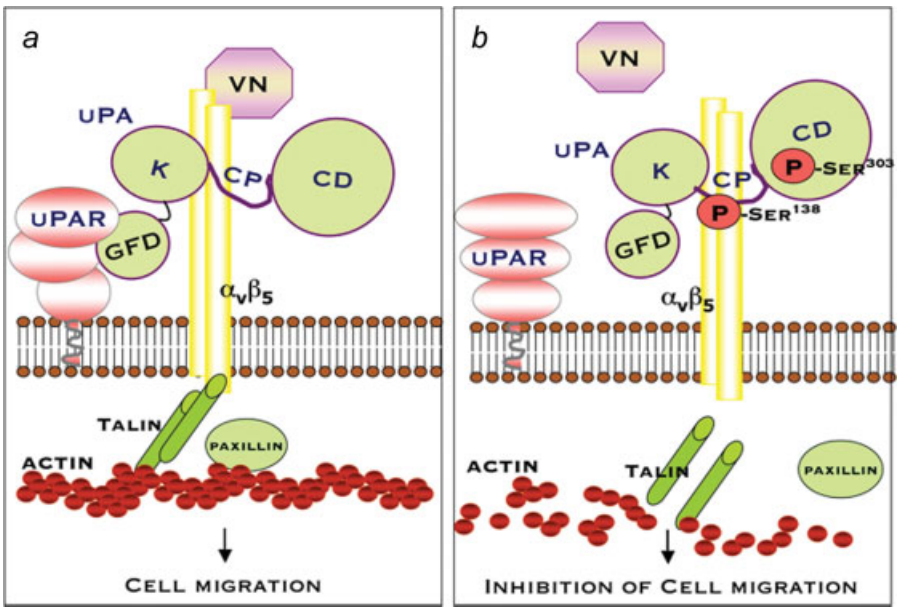

FIGURE 7 – Model for inhibition of cell migration by phospho-uPA. Our data show that the CP region of uPA binds with high affinity to αvβ5 integrin, independently of the phosphorylation state of $Ser^{138/303}$. Unphosphorylated uPA stimulates uPAR/αvβ5 colocalization and enhances β5-talin association and F-actin polymerization, thus resulting in lamellipodia formation and in the enhancement of cell migration (panel *a*). In contrast, phospho-uPA prevents uPAR/αvβ5 association, weakens the β5-talin physical connection, reduces actin polymerisation, decreases αvβ5 affinity for VN and impairs cell response to VN, leading to a general inhibition of cell migration (panel *b*).

The ultimate step in the activation of most integrins is believed to be its interaction, through the NpxY motif in the cytoplasmic tail, with talin.[32] We investigated whether the $\Delta GFa^{138E/303E}$ interaction with αvβ5 might result in a reduced ability to bind talin. HEK-293/αv cl.38 cells, which express high level of αv, were grown on VN-coated dishes exposed to $\Delta GFa^{138E/303E}$, lysed, immunoprecipitated with an anti-β5 antibody and immunoblotted with anti-talin antibody. As shown in Figure 6*c*, compared with control, VN-adherent cells had increased talin/β5 association, which was reduced when cells were incubated with $\Delta GFa^{138E/303E}$. These results indicate that the phosphorylation state of uPA indirectly downregulates αvβ5 integrin affinity for VN and β5 ability to interact with talin.

Discussion

We provide evidence that specific phosphomimic variants of human uPA (uPA^{138E}, $\Delta GFa^{138E/303E}$ and $uPA^{138E/303E}$) are strong inhibitors of carcinoma cell migration and invasion *in vivo*. These uPA variants, which are the engineered forms of naturally occurring, phosphorylated forms of uPA,[22] reduce speed of cell translocation and prevent the formation of F-actin-enriched lamellipodia-like structures, which drive cell locomotion. Phosphomimic uPA variants bind to αvβ5 integrin, reduce its state of activation, as evidenced by a decreased β5-talin intracellular association, and downmodulate its affinity for VN. These data reveal an unsuspected inhibitory function of phosphorylated or Glu-substituted uPA and suggest that these protease variants may interfere with a crucial mechanism required for cell locomotion (Fig. 7).

The finding that uPA^{138E} retains most of the inhibitory ability of the disubstituted variants supports a major regulatory role for the CP region of uPA, surrounding Ser^{138}. The functional relevance of the 132–158 region was first suggested by the analysis of uPA serine phosphorylation. In A431 human carcinoma cells, a proportion of endogenously produced uPA is phosphorylated on Ser^{138} and/or Ser^{303}.[22] Interestingly, Ser^{138} is conserved among most mammal species, including mouse, rat, yellow baboon, bovine and orangutan, supporting an important functional role (Votta and Stoppelli, unpublished). Further evidence indicating the importance of the CP region is based on the effects of Å6, a capped 8 amino acid peptide (KKPSSPPEE), corresponding to uPA residues 135–143, which inhibits tumor progression and angiogenesis.[33] The clear-cut ability of Å6 to prevent tumor growth and metastasis in models of glioblastoma, breast and prostate cancer led to its use in phase I trials for anti-cancer therapy.[34] Interestingly, our recent study shows that an isolated peptide corresponding to uPA residues 135–158, and therefore including the Å6 sequence, binds to αvβ5 integrin with high affinity, is chemotactic at picomolar concentrations and stimulates the colocalization of uPAR and αvβ5 integrin.[19]

The cryptic activity of protease domains is not unique to uPA, as it has been described for other multidomain proteases. One example is the naturally occurring C-terminal hemopexin-like domain of MMP-2 named PEX, which prevents this enzyme binding to αvβ3, thus blocking cell-surface MMP-2 activity, angiogenesis and tumor growth.[35] Several antiangiogenic factors are derived from proteolytic processing of large molecules.[36] Interestingly, the isolated kringle region of uPA also exhibits some growth-inhibitory activity; in the report by Kim *et al.*,[37] a recombinant kringle (UK1, residues 47–135 of human uPA) was shown to inhibit endothelial cell proliferation stimulated by bFGF, VEGF or EGF in a uPAR-independent manner. A thorough understanding of the mechanism of action of potential antiinvasive agents is required to develop efficient antimetastatic therapies as well as aiding in the rational application of combination therapies. Among integrins, the αvβ3 and αvβ5 receptors are regarded as important therapeutic targets for anti-angiogenic and antimetastatic therapies. Cilengitide (cyclic peptidic integrin αvβ3/αvβ5 antagonist) is currently in clinical trials for antiangiogenic cancer therapy.[38]

Phosphomimic uPA, at picomolar concentrations, interacts with αvβ5 through its CP region, similar to wild-type unphosphorylated uPA[19] with Kdapp as low as 1–10 pM. However, the interaction with the phosphomimic affects cell behavior differently (Fig. 7). First, it increases the VN concentration required for stimulation of cell migration by 10- to 100-fold. Second, it weakens the physical connection between integrin and the cytoskeleton-associated talin. Third, it changes the localization of F-actin inhibiting the

protruding structures observed in cells exposed to wild-type uPA. Finally, it reduces cell speed by 5-fold and severely affects invasion of cancer cells in the CAM model. The most ready interpretation of these observations is that the CP region of uPA, carrying Ser^{138}, induces a unique conformational change of αvβ5 integrin, which prevents its ligand-dependent increase in affinity and disrupts its physical connection to cell cytoskeleton. As a result, integrin occupancy is reduced and cell response to VN is impaired. It has been shown previously that αvβ5-dependent cell migration is regulated by the ectodomain of the β subunit.[39] These authors suggested that sequences within the ectodomain might influence the packing of the integrin in the plane of the membrane or its lateral associations. It is possible that binding of the disubstituted uPA affects these interactions, resulting in a blockade of integrin function. Although, we do not yet have an explanation for the general inhibition of cell migration/adhesion to matrix proteins other than VN. It is possible that the changes induced by the phosphomimics in the cytoskeleton (F-actin) are incompatible with migration. Moreover, we found that binding of the inhibitory uPA-variants to αvβ5 affects ligand interaction with other integrin receptors (not shown), suggesting that αvβ5 inactivation may extend to other integrins through an inside-out signaling. Further work is needed to dissect the molecular pathway/s and signaling events responsible for these effects.

Overall, our data shed new light on the function of uPA, a protein causally involved in human cancer.[1] Based on the current and previously published data,[19] we conclude that a specific region of uPA, the CP, interacts with cell-surface αvβ5 integrin and, depending on the state of phosphorylation of Ser^{138} in CP, either stimulates or blocks cell migration (Fig. 7). Importantly, the finding that uPAs, or shorter segments of uPA that include phosphomimic of Ser^{138}, are such potent inhibitors of cell migration and invasion opens new opportunities for clinical anticancer applications. Moreover, the CP/integrin interaction and its downstream molecular sequel might represent a new paradigm in search for agents aimed at inhibition of cancer cell invasion.

References

1. Andreasen PA, Kjoller L, Christensen L, Duffy MJ. The urokinase-type plasminogen activator system in cancer metastasis: a review. Int J Cancer 1997;72:1–22.
2. Shariat SF, Roehrborn CG, McConnell JD, Park S, Alam N, Wheeler TM, Slawin KM. Association of the circulating levels of the urokinase system of plasminogen activation with the presence of prostate cancer and invasion, progression, and metastasis. J Clin Oncol 2007;25:349–55.
3. Pillay V, Dass CR, Choong PF. The urokinase plasminogen activator receptor as a gene therapy target for cancer. Trends Biotechnol 2007;25:33–9.
4. Huai Q, Mazar AP, Kuo A, Parry GC, Shaw DE, Callahan J, Li Y, Yuan C, Bian C, Chen L, Furie B, Furie BC, et al. Structure of human urokinase plasminogen activator in complex with its receptor. Science 2006;311:656–59.
5. Llinas P, Le Du MH, Gardsvoll H, Dano K, Ploug M, Gilquin B, Stura EA, Ménez A. Crystal structure of the human urokinase plasminogen activator receptor bound to an antagonist peptide. EMBO J 2005;24:1655–63.
6. Kjaergaard M, Hansen LV, Jacobsen B, Gardsvoll H, Ploug M. Structure and ligand interactions of the urokinase receptor (uPAR). Front Biosci 2008;13:5441–61.
7. Ossowski L, Aguirre-Ghiso JA. Urokinase receptor and integrin partnership: coordination of signaling for cell adhesion, migration and growth. Curr Opin Cell Biol 2000;12:613–20.
8. Wei Y, Yang X, Liu Q, Wilkins JA, Chapman HA. A role for caveolin and the urokinase receptor in integrin-mediated adhesion and signaling. J Cell Biol 1999;144:1285–94.
9. Hynes RO. Integrins: bidirectional, allosteric signaling machines. Cell 2002;110:673–87.
10. Aguirre Ghiso JA, Kovalski K, Ossowski L. Tumor dormancy induced by downregulation of urokinase receptor in human carcinoma involves integrin and MAPK signaling. J Cell Biol 1999;147:89–104.
11. Carriero MV, Del Vecchio S, Capozzoli M, Franco P, Fontana L, Zannetti A, Botti G, D'Aiuto G, Salvatore M, Stoppelli MP. Urokinase receptor interacts with α (v) β 5 vitronectin receptor, promoting urokinase-dependent cell migration in breast cancer. Cancer Res 1999; 59:5307–14.
12. Wei Y, Lukashev M, Simon DI, Bodary SC, Rosenberg S, Doyle MV, Chapman HA. Regulation of integrin function by the urokinase receptor. Science 1996;273:1551–55.
13. Liu D, Aguirre Ghiso J, Estrada Y, Ossowski L. EGFR is a transducer of the urokinase receptor initiated signal that is required for *in vivo* growth of a human carcinoma. Cancer Cell 2002;1:445–57.
14. Montuori N, Carriero MV, Salzano S, Rossi G, Ragno P. The cleavage of the urokinase receptor regulates its multiple functions. J Biol Chem 2002;277:46932–39.
15. Wei Y, Czekay RP, Robillard L, Kugler MC, Zhang F, Kim KK, Xiong JP, Humphries MJ, Chapman HA. Regulation of α5β1 integrin conformation and function by urokinase receptor binding. J Cell Biol 2005;168:501–11.
16. Silvestri I, Longanesi Cattani I, Franco P, Pirozzi G, Botti G, Stoppelli MP, Carrieo MV. Engaged urokinase receptors enhance tumor breast cell migration and invasion by upregulating α(v)β5 vitronectin receptor cell surface expression. Int J Cancer 2002;102:562–71.
17. Lijnen HR, Van Hoef B, Collen D. Activation with plasmin of two-chain urokinase-type plasminogen activator derived from single-chain urokinase-type plasminogen activator by treatment with thrombin. Eur J Biochem 1987;169:359–64.
18. Appella E, Robinson EA, Ullrich SJ, Stoppelli MP, Corti A, Cassani G, Blasi F. The receptor-binding sequence of urokinase. A biological function for the growth-factor module of proteases. J Biol Chem 1987;262:4437–40.
19. Franco P, Vocca I, Carriero MV, Alfano D, Cito L, Longanesi-Cattani I, Grieco P, Ossowski L, Stoppelli MP. Activation of urokinase receptor by a novel interaction between the connecting peptide region of urokinase and alphavbeta5 integrin. J Cell Sci 2006;119:3424–34.
20. Degryse B, Orlando S, Resnati M, Rabbani SA, Blasi F. Urokinase/urokinase receptor and vitronectin/α(v)β(3) integrin induce chemotaxis and cytoskeleton reorganization through different signaling pathways. Oncogene 2001;20:2032–43.
21. Sturge J, Hamelin J, Jones GE. N-WASP activation by a beta1-integrin-dependent mechanism supports PI3K-independent chemotaxis stimulated by urokinase-type plasminogen activator. J Cell Sci 2002;115:699–711.
22. Franco P, Iaccarino C, Chiaradonna F, Brandazza A, Iavarone C, Mastronicola MR, Nolli ML, Stoppelli MP. Phosphorylation of human pro-urokinase on Ser138/303 impairs its receptor-dependent ability to promote myelomonocytic adherence and motility. J Cell Biol 1997;137:779–91.
23. Franco P, Massa O, Garcia-Rocha M, Chiaradonna F, Iaccarino C, Correas I, Mendez E, Avila J, Blasi F, Stoppelli MP. Protein kinase C-dependent *in vivo* phosphorylation of prourokinase leads to the formation of a receptor competitive antagonist. J Biol Chem 1998; 273:27734–40.
24. Carriero MV, Franco P, Gargiulo L, Vocca I, Cito L, Fontana L, Iaccarino C, Del Pozzo G, Guardiola J, Stoppelli MP. Inhibition of receptor-dependent urokinase signaling by specific Ser to Glu substitutions. Biol Chem 2002;383:107–13.
25. Toolan HW. Transplantable human neoplasms maintained in cortisone-treated laboratory animals: H.S. No. 1; H.Ep. No. 1; H.Ep. No. 2; H.Ep. No. 3; and. H.Emb. Rh. No. 1. Cancer Res 1954;14:660–6.
26. Ossowski L, Reich E. Experimental model for quantitative study of metastasis. Cancer Res 1980;40:2300–9.
27. Ossowski L, Russo H, Gartner M, Wilson EL. Growth of a human carcinoma (HEp3) in nude mice: rapid and efficient metastasis. J Cell Physiol 1987;133:288–96.
28. Stoppelli MP, Tacchetti C, Cubellis MV, Corti A, Hearing VJ, Cassani G, Appella E, Blasi F. Autocrine saturation of pro-urokinase receptors on human A431 cells. Cell 1986;45:675–84.
29. Tranquillo RT, Lauffenburger DA, Zigmond SH. A stochastic model for leukocyte random motility and chemotaxis based on receptor binding fluctuations. J Cell Biol 1988;106:303–9.
30. Ossowski L. *In vivo* invasion of modified chorioallantoic membrane by tumor cells: the role of cell surface-bound urokinase. J Cell Biol 1988;107:2437–45.
31. Liddington RC, Ginsberg MH. Integrin activation takes shape. J Cell Biol 2002;158:833–39.
32. Tadokoro S, Shattil SJ, Eto K, Tai V, Liddington RC, de Pereda JM, Ginsberg MH, Calderwood DA. Talin binding to integrin beta tails: a final common step in integrin activation. Science 2003;302:103–6.
33. Guo Y, Higazi AA, Arakelian A, Sachais BS, Cines D, Goldfarb RH, Jones TR, Kwaan H, Mazar AP, Rabbani SA. A peptide derived from the nonreceptor binding region of urokinase plasminogen activator

(uPA) inhibits tumor progression and angiogenesis and induces tumor cell death *in vivo*. FASEB J. 2000;14:1400–10.
34. Berkenblit A, Matulonis UA, Kroener JF, Dezube BJ, Lam GN, Cuasay LC, Brünner N, Jones TR, Silverman MH, Gold MA. A6, a urokinase plasminogen activator (uPA)-derived peptide in patients with advanced gynecologic cancer: a phase I trial. Gynecol Oncol 2005;99:50–7.
35. Brooks PC, Silletti S, von Schalscha TL, Friedlander M, Cheresh DA. Disruption of angiogenesis by PEX, a noncatalytic metalloproteinase fragment with integrin binding activity. Cell 1998;92:391–400.
36. Bix G, Iozzo RV. Matrix revolutions: "tails" of basement-membrane components with angiostatic functions. Trends Cell Biol 2005;15:52–60.
37. Kim KS, Hong YK, Joe YA, Lee Y, Shin JY, Park HE, Lee IH, Lee SY, Kang DK, Chang SI, Chung SI. Anti-angiogenic activity of the recombinant kringle domain of urokinase and its specific entry into endothelial cells. J Biol Chem 2003;278:11449–56.
38. Nabors LB, Mikkelsen T, Rosenfeld SS, Hochberg F, Akella NS, Fisher JD, Cloud GA, Zhang Y, Carson K, Wittemer SM, Colevas AD, Grossman SA. Phase I and correlative biology study of cilengitide in patients with recurrent malignant glioma. J Clin Oncol 2007;25:1651–7.
39. Filardo EJ, Deming SL, Cheresh DA. Regulation of cell migration by the integrin beta subunit ectodomain. J Cell Sci 1996;109:1615–22.